Low-budget light-enhanced NMR spectrometer

Dr. Takuya Segawa, ETH Zürich

1. Summary of the research plan

Nuclear Magnetic Resonance (NMR) spectroscopy is one of the most versatile and powerful analytical tools for chemistry, biology, pharmaceutical or material sciences. At the same time, NMR is an ideal playground to experience quantum mechanics “with own hands”. Even though almost 80 years old, the MR science and technology is barely present in the “Global South” due to its extremely high costs and the need for a continuous supply of liquid helium. To counteract this inequality, our project is to develop and construct a low-field light-enhanced NMR spectrometer for academia of the “Global South”. The spectrometer will be controlled using a mobile phone app. The final product, once produced in larger quantities, should not cost more than CHF 10’000. The whole endeavor will be fully noncommercial and open source.

Our spectrometer will be based on a highly homogeneous cryogen-free permanent magnet in a field range of 0.5 – 1.5 T, corresponding to a ^{1}H NMR Larmor frequency of ca. 20 – 60 MHz. An actively shimmed permanent magnet at 0.6 T with a homogeneity corresponding to a ^{1}H NMR linewidth of 2.5 Hz at 25 MHz, developed by an expert company, will be readily available at the start of the project. To boost the NMR signal strength, a high-power LED (costing a few Swiss Francs) will induce photochemically-induced dynamic nuclear polarization (photo-CIDNP) to hyperpolarize nuclear spins in aromatic molecules. Photo-CIDNP is our method of choice for NMR signal enhancement since it is by far the simplest and cheapest hyperpolarization technique for liquid-state NMR spectroscopy at low fields. Besides hardware and software development, the project will focus on automatization for NMR measurements (magnet temperature control, field/frequency lock, shimming, etc.) under these low-field conditions to guarantee the accessibility for NMR beginners. To overcome the inherent limit in resolution due to the small chemical shift dispersion at low magnet fields, we will develop experimental and processing techniques to simplify the spectra and increase their chemical information content, also relying on recent neural network-based approaches. In a second step, incorporating the experience from the initial spectrometer prototype at 0.6 T, a second NMR spectrometer at a higher field (e.g., ca. 1 T) will be designed and constructed. We will explore potential chemical and biological applications on our low-field spectrometer for education and research using photo-CIDNP NMR spectroscopy. At the end of the project, a prototype spectrometer will be contributed to a university of the “Global South” to initiate a partnership. The outcome of our project will be the starting point for the non-profit production of the light-enhanced low-field NMR spectrometer.

2. Research plan

2.1. Current state of research in the field

Our project is inspired by and based on five topical aspects, whose state of knowledge will be described in this section:

1) Photo-CIDNP NMR spectroscopy for biological and pharmaceutical studies
2) Low-field NMR spectroscopy using a permanent magnet
3) Hyperpolarization combined with low-field magnetic resonance
4) Open-source NMR spectrometers and MRI scanners
5) Accessible NMR spectrometers for the "Global South"

2.1.1. Photo-CIDNP NMR spectroscopy for biological and pharmaceutical studies

NMR signal enhancement of specific amino acid residues in solution-state NMR spectroscopy, when exciting an added dye with visible laser light, were developed by Kaptein et al. in the 1978.[1] Most notably, the pioneering paper described an application in the, at that time very young field of, protein NMR spectroscopy, where the photo-CIDNP effect revealed the difference between water-exposed and buried aromatic amino acid residues. Based on this, photo-CIDNP was and is still used[2] as a method to highlight structural details in biomolecules,[3] rather than a tool for hyperpolarization to improve the signal-to-noise ratio (SNR) in NMR spectroscopy.

In the last two decades when hyperpolarization became a central topic in NMR method development, the research groups of Lucio Frydman[4], Silvia Cavagnero[5,6] and Roland Riek (project partner)[7–9] promoted photo-CIDNP as a mechanism for NMR signal enhancement. Recently, Mompeán at al. combined photo-CIDNP with microfluidics/microcoil NMR to detect a sample volume of only 1 μL.[10] As a key step, the group of Cavagnero presented a combination of three enzymes acting as protection against the photodegradation of dye and other molecules, a main drawback of the photo-CIDNP method in need of high laser power, enabled to reach signals of molecules at low micromolar range.[11] Furthermore, the research group widened up the potential candidates for photo-CIDNP dyes by demonstrating the efficiency of fluorescein, a cheap and readily available organic dye molecule.[12] By demonstrating its strong photo-CIDNP enhancement, the Riek group added the dye Atto Thio 12 as a new choice for a photosensitizer.[7] In the same work, they showed that cost-efficient laser diodes can be coupled into multimode fibers, which then directly guide the light into the solution of the NMR tube.[7] Besides opening the chemical space for the dye molecules, Torres et al. of the Riek lab showed the potential of a vast quantity of small molecules with currently unknown photo-CIDNP activity. As an impressive example, the oxidation product of tryptophan, 3α-hydroxypyrroloindole, showed an unprecedented photo-CIDNP enhancement of 380-fold at 200 MHz.[8] All these findings proof that a smart combination of photosensitizer dye, molecule of interest and magnetic field strength can lead to stronger hyperpolarization than previously observed in photo-CIDNP NMR spectroscopy.[9]

As a novel application of photo-CIDNP, Torres et al. proposed a highly accelerated drug screening method based on NMR. By compiling a chemical library of photo-CIDNP active ligand molecules, photo-CIDNP NMR spectra of

a ligand is studied in absence and presence of a target protein. If these spectra show a difference due to hindered photo-CIDNP polarization of the ligand caused by protein-ligand binding, a "hit" is reported. The patent for this invention was ranked among the Top 5 of this year's ETH Spark Award[13] and the idea led to the founding of the start-up company NexMR.[14]

2.1.2. Low-field NMR spectroscopy using a permanent magnet

For a long time, the development of new NMR spectrometers only knew a single direction: higher and higher magnetic fields. This is well justified by the improved SNR (scaling with ${B_0}^{3/2}$, where B_0 is the magnetic field strength in Tesla)[15] and spectral resolution (dispersion of chemical shift scaling with B_0). In recent years, a non-negligeable niche started to flourish: the benchtop NMR spectrometer at low fields (corresponding to a ^{1}H NMR Larmor frequency below 100 MHz), which was pioneered by Bernhard Blümich and others.[16] Due to the challenging magnetic field homogeneity, initial experiments focused on "relaxometry" applications, where relaxation curves were observed without resolving chemical shifts. Today, different commercial suppliers offer NMR spectrometers with linewidths allowing for impeccable chemical analysis of small molecules, for example the Spinsolve series (Magritek, Germany/New Zealand)[17] offering spectrometers between 60-90 MHz ^{1}H NMR Larmor frequency or the Fourier 80 spectrometer (Bruker, USA/Germany/Switzerland)[18] at a ^{1}H NMR Larmor frequency of 80 MHz. Earlier this year, the first benchtop NMR spectrometer QM-125 (Q Magnetics, USA)[19] based on a permanent magnet reaching a ^{1}H NMR Larmor frequency of 125 MHz was presented. The prices range from ca. CHF 40'000 to CHF 100'000 and higher. Besides the lower acquisition costs, the absence of cryogenics and the compact size are the key advantages. Current "standard" magnetic fields for benchtop NMR spectrometers are corresponding to around 60-80 MHz ^{1}H NMR Larmor frequency.

2.1.3. Hyperpolarization combined with low-field magnetic resonance

As mentioned above, the limitation of low-field[1] to high-field NMR spectra are the insufficient chemical shift dispersion, leading to signal overlap, and the small SNR. While the former can only be adjusted by changing the gyromagnetic ratio and therefore the observed nuclei (for example switching from ^{1}H to ^{13}C, which enlarges the chemical shift range by one order of magnitude), for the latter, an obvious solution to boost the signal is hyperpolarization.[20] Before arriving at NMR spectroscopy, this combination was first explored in the area of low-field magnetic resonance imaging (MRI), where fields around 1 T are still common, due to the much larger sample size. Hyperpolarization of noble gases induced by optical pumping and spin exchange, was pioneered for lung imaging in mice as early as 1994.[21] The SNR of hyperpolarized MRI at low fields was theoretically studied and for the case of sample noise dominating over coil noise, a behavior that is largely independent of magnetic field and frequency was found.[22] This decoupling of SNR and magnetic field strength must be seen as a paradigm

[1] With low-field NMR, herein we define a ^{1}H NMR frequency range of < 100 MHz, which should not be confused with zero- and ultra-low (ZULF) NMR spectroscopy,[74] where the chemical shift is negligeable or much smaller than the *J*-couplings.

change in magnetic resonance: Higher magnetic fields now only improve the spectral resolution (larger dispersion of chemical shift), but not anymore (or only weakly) the SNR.

In the following, we present the readily available hyperpolarization techniques and evaluate them regarding their combination with low-field NMR spectroscopy.

SABRE:

For low-field benchtop NMR spectroscopy, Signal Amplification By Reversible Exchange (SABRE)[23] appears to be the most convenient and efficient hyperpolarization method today. SABRE relies on enriched parahydrogen (*p*-H_2) as a source of nuclear spin polarization. The group of Meghan Halse showed impressive results at ^{1}H NMR Larmor frequency of 43 MHz ($B_0 = 1$ T), reaching a spin polarization of up to 5.9 % (17'000-fold enhancement) for ^{1}H and up to 4 % (45'500-fold enhancement) ^{13}C NMR signals including ^{1}H 2D spectra.[24] In their work, *p*-H_2 was produced either by cooling "normal" H_2 to 28 K or 38 K, leading to a *p*-H_2 enrichment of 98 % and 92 %, respectively. SABRE is chemically specific and only works for molecules, which allow for a reversible exchange with *p*-H_2. An advantage over other hyperpolarization methods like dissolution dynamic nuclear polarization (dDNP, see below) is the continuous generation (rather than "single shot") of non-thermal spin polarization.[20]

Dissolution DNP:

The group of Sami Jannin demonstrated ^{13}C NMR spectra at a 80 MHz (^{1}H NMR Larmor frequency, $B_0 \approx 2$ T), benchtop NMR spectrometer after dDNP with an enhancement of up to four orders of magnitude in S/N to thermal polarization.[25] In the case of dDNP, stable radicals/unpaired electrons are the source of hyperpolarization. The setup requires a polarizer consisting of a separate superconducting magnet (up to 7 T), the sample cooled down to liquid Helium temperature as well as microwave and radiofrequency irradiation for the electron to nuclear spin polarization transfer.[26] After the DNP process in the frozen state, the sample is dissolved by boiling water and transferred to the liquid-state NMR spectrometer. dDNP is technically much more complex and expensive than SABRE, but achieves hyperpolarization of almost all small molecules.[27] Larger molecules such as proteins do not survive the harsh conditions of the dissolution process.

Overhauser DNP:

A further method, which achieves hyperpolarization of the liquid NMR sample is Overhauser DNP. Thorsten Maly and co-workers obtained enhancement factors of >30 at a ^{1}H Larmor frequency of 14.5 MHz ($B_0 = 0.35$ T).[28] These enhancement factors are more than two orders of magnitude lower than for the previously mentioned hyperpolarized techniques SABRE and dDNP. As an additional disadvantage the presence of radicals in the solutions broadens the NMR lines, which ultimately limits the spectral resolution. From the hardware side, a high-power microwave source (10 W) is needed, which may introduce heating of the liquid sample. On the other hand, the advantage of Overhauser DNP is that it is a room temperature polarization technique and does not rely on cryogenics opposed to SABRE and dDNP.

Photo-CIDNP:

In 2022, Bernarding et al. demonstrated a nice combination of photo-CIDNP on ^{19}F NMR and MRI at a magnetic field of 0.6 T,[29] using the educational low-field benchtop MRI device "magspec" (Pure Devices, Germany).[30] As a high-power light source, they used an inexpensive LED (only a few CHF) to polarize a fluorinated tyrosine using riboflavin 5'-monophosphate (FMN) as a photosensitizer dye. ^{19}F NMR has the convenient advantage that the Larmor frequency is close to ^{1}H spins, but the absence of the strong solvent water signals allows a background-free acquisition. However, since the device was designed for imaging, the linewidth was limited by the magnetic field inhomogeneity to about 20 Hz (FWHM, estimated from Fig. 3 in Ref. [29]), preventing high-quality chemical analysis. The estimated signal enhancement was almost 500, being one order of magnitude above Overhauser DNP, but still more than one order of magnitude below SABRE and dDNP. The field/frequency stability was guaranteed by locking on the ^{1}H NMR signal of water on a second radiofrequency signal channel. Similar to SABRE, the polarizable molecules are chemically limited by the formation of radical pairs with the dye molecule (mostly containing aromatic groups).[3] The authors declared the cost of the total setup as "well below EUR 100'000".

2.1.4. Open-source NMR spectrometers and MRI scanners

Today, most NMR spectrometers and MRI scanners are fully commercial devices. This includes the operating software to run experiments, which is also proprietary and not open source. This situation has two major drawbacks: First, NMR users have become dependent of the setup manufacturers. Second, the NMR spectrometer has become a black box, which cannot anymore be repaired by scientists and, most importantly, does not anymore allow to instruct students about instrumentation.

It was Kazuyuki Takeda who launched an independent and fully open-access NMR console called Opencore NMR[31] as early as 2007.[32,33] The heart of his system is a field-programmable gate-array (FPGA) on a chip (a few millimeters each side), which digitally fulfills the key tasks; the whole NMR console board has about the size of an A4 page replacing a hardware unit taller than 1 m in a commercial high-field NMR spectrometer! All plans for the circuit board manufacturing of an Opencore NMR system are publicly available and open source.[33] Today, Takeda's systems are distributed over the whole world, including MR research at ETH Zürich (groups of Matthias Ernst and Sebastian Kozerke).[34] Besides the FPGA-based console, Takeda also provides a software to run experiments on Opencore NMR systems and to process the acquired data (both written in C++), which are available for Linux, Mac and Windows systems. The cost for the latest Opencore NMR console is stated to be EUR 5000 and can be used on a high-field NMR spectrometer with a ^{1}H Larmor frequency of up to 600 MHz ($B_0 = 14$ T).[35] Takeda's Opencore NMR systems have so far been used in the field of solid-state NMR spectroscopy, where hardware development is still more vivid than in solution-state NMR.

In 2016, Lukas Winter and others initialized the open source imaging initiative to make hardware and software for medical MRI open source.[36] Since the start, almost one hundred projects have been added and an online community of three hundred people (members of the dedicated Slack channel) was built up. The vision of this initiative is to publicly share the knowhow on MRI software and hardware and thereby increase the accessibility

to medical MRI. One of the project is the MAgnetic Resonance Control System - MaRCoS, an open-source electronic control system for low-field MRI realized by a collaboration of scientist from five different countries.[37] MaRCoS is an MRI console, which is based on a commercially radiofrequency (RF) board the SDRLab 122-16 (Red Pitaya, Slovenia) with a Xilinx Zynq 7020 FPGA.[38] The SDRLab 122-16 has an even more compact size of a credit card, two RF inputs (16-bit resolution) and two outputs (14-bit resolution), generates RF frequencies up to 122.88 MHz and costs EUR 500. The device falls into the category of software-defined radio (SDR): a radio system where traditional analog components are replaced by digital components and software technologies.[39] This leads to a drastic reduction in size and price and makes the systems more general. Recently, Carl Michal proposed a similar NMR console, based on LimeSDR (12-bit resolution).[40] The whole MaRCoS system architecture is shown in Figure 1. The MaRCoS console was successfully used in MRI scanners with fields ranging from 50 mT to 360 mT.[41]

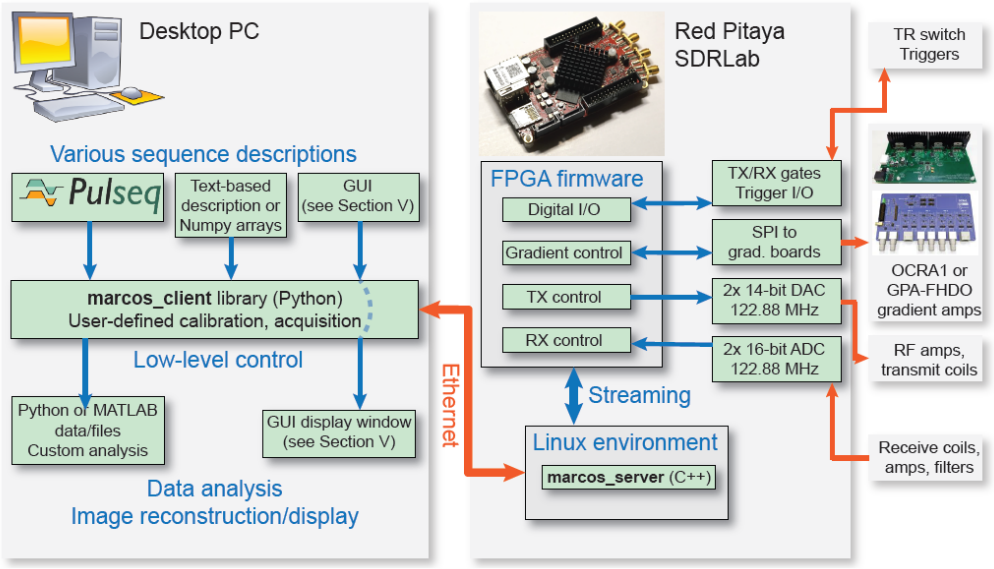

Figure 1. System architecture of the open-source MRI console MaRCoS. The system is controlled via a Desktop PC (left), using a Python-based software. On the SDRLab (center), a C++-based server is running on an exchangeable SD card. The PC and the SDRLab are connected by a Ethernet cable. The SDRLab controls the RF hardware and magnetic field gradients for MRI. Reprinted from arXiv publication.[37]

2.1.5. Accessible NMR spectrometers for the "Global South"

To the best of our knowledge, to date, we are not aware of any initiative, in Switzerland or worldwide, to specifically create a low-budget and accessible NMR spectrometer for the "Global South" (see Figure 8 for the detailed map of target countries). This project will answer the research question, how to provide an NMR spectrometer guaranteeing a high functionality for education and research by, at the same time, limiting the production costs. Our approach is a combination of a low-field permanent magnet (0.5 – 1.5 T / 20 – 80 MHz ^{1}H NMR frequency) as a key part of a cheap and compact NMR spectrometer (thanks to new readily available RF devices). The weak NMR signal will be boosted by hyperpolarization relying on photo-CIDNP, which only needs

a high-power LED (cost: a few CHF) as additional hardware. The limited resolution (small chemical shift dispersion) will be counteracted by experimental and processing steps to simplify spectra, including recent advances based on deep neural networks. Today, construction of liquid-state NMR spectrometers take almost exclusively place in commercial companies. A goal of our project is to keep this knowledge open and accessible, especially for researchers in the "Global South".

2.2. Current state of own research

After five years of research as a Branco Weiss Fellow with a focus on optically-polarized electron triplet states in Nitrogen-Vacancy (NV) centers in diamond and organic crystals such as pentacene for NMR hyperpolarization,[42] including the construction of a wide-field fluorescence microscope for optically-detected magnetic resonance, the applicant joined the Riek lab in February 2022 to continue his research on photo-CIDNP hyperpolarization for biological NMR spectroscopy.

2.2.1. Photo-CIDNP-enhanced low-field NMR spectroscopy

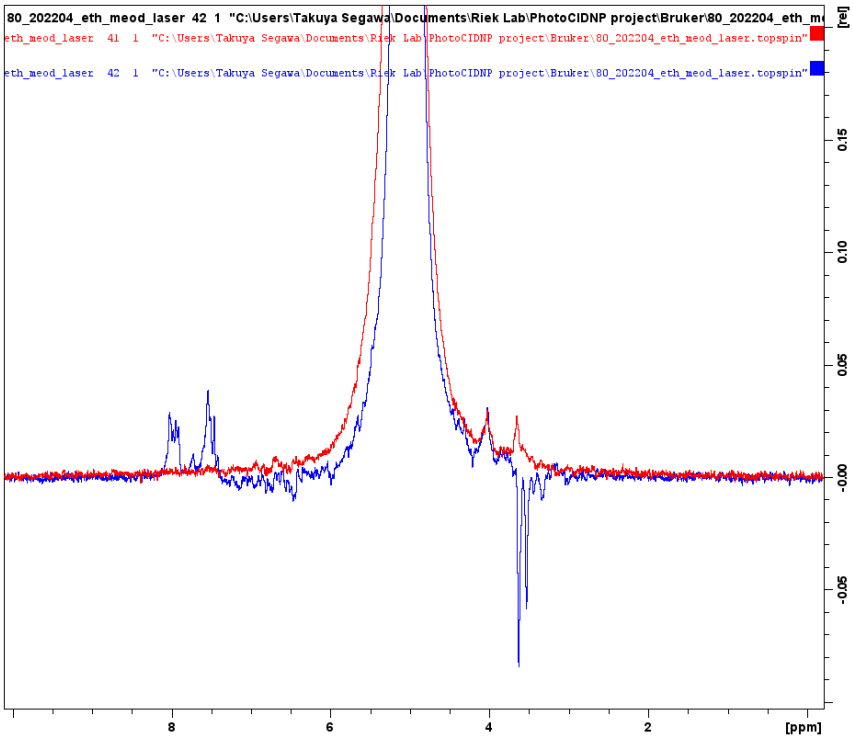

Figure 2. ^{1}H NMR spectra of 100 µM tryptophan and 25 µM fluorescein with the enzyme system GO-CAT[11] recorded at 80 MHz using a benchtop spectrometer (Fourier 80, Bruker). The red trace shows the signal without, the blue trace with laser irradiation. The positively enhanced ^{1}H signals in the range of 7-9 ppm are aromatic protons, the negatively enhanced signals around 3 ppm are aliphatic protons of tryptophan. The two peaks around 4 ppm, present in the "dark" spectra are protons from glucose (5 mM), used to quench the oxygen. The spectra were recorded by averaging over four scans for 1 minute. The solvent was pure H_2O without the addition of D_2O. Water suppression was implemented using a composite pre-saturation pulse (Bruker pulse sequence: zgcppr). The laser used for optical excitation was a diode laser emitting at 450 nm (L450P1600MM, Thorlabs). The laser light was guided into an optical fiber, which ended directly inside the liquid sample of the NMR tube as described by Torres et al.[8,9] We thank Dr. Barbara Czarniecki (Bruker, Fällanden) for experimental help.

Relying on the previously accomplished methodological achievements in the Riek group (see section 2.1),[7–9,13] we tested the photo-CIDNP enhancement on a low-field benchtop NMR spectrometer. Figure 2 shows preliminary results of a photo-CIDNP ^{1}H NMR spectrum recorded at 80 MHz using a Fourier 80 spectrometer (Bruker). Using a sample of 100 μM tryptophan and 25 μM fluorescein as photosensitizer dye, aromatic (ca. 7-9 ppm, positive enhancement) and aliphatic protons (around 3 ppm, negative enhancement) became clearly visible under laser irradiation (Figure 2 blue trace), which were not detectable in a conventional NMR acquisition without light (Figure 2 red trace). The addition of the enzyme system GO-CAT (glucose oxidase and catalase)[11] prevented the dye molecule from fast bleaching. The acquisition time for the photo-CIDNP experiment was about 1 minute, where the conventional acquisition took about 24 hours to reach the same SNR. This fast acquisition is a strong advantage to minimize the temperature induced magnetic field drifts of the permanent magnet (see discussion below). The Besides fighting a low SNR, the challenge using aqueous sample is to see the very dilute signals (ppm in concentration) despite the huge water NMR signal. Using a 100% H_2O sample (no deuterated solvent) the water suppression of the Fourier 80 fulfills this task impressively by using a composite pulse pre-saturation on water. This experiment was an initial trial with a manual switching of the laser and not yet optimized, but shows that sub-millimolar detection of photo-CIDNP-enhanced ^{1}H-NMR is readily achievable.

2.2.2. MaRCoS on SDRLab 122-16: A compact and cheap NMR console

To evaluate the performance of the SDRLab 122-16 as a console for a low-field NMR spectrometer, we purchased the board and installed MaRCoS server on a SD card and the MaRCoS client on a windows computer following the instructions.[43] Since the software was designed for Linux systems, a Windows Subsystem for Linux (WSL) running ArchLinux was implemented on a Windows machine. The SDRLab 122-16 (see Figure 3) running on MaRCoS successfully generated an RF pulse at a frequency of 24.46 MHz (corresponding to a ^{1}H Larmor frequency at $B_0 \approx 0.6$ T) with a duration of 80 μs, which was detected with an oscilloscope (see Figure 4). Vice versa, we generated with an RF signal generator a signal at 5.01 MHz, while setting the local oscillator (LO) frequency in the SDRLab 122-16/MaRCoS system to 5 MHz. The console detected the down-converted complex signal of 10 kHz, which is plotted using Python in Figure 5. These two simple experiment demonstrate that the SDRLab 122-16/MaRCoS system is suitable as a console for a NMR system of up to 60 MHz (ca. 1.5 T for ^{1}H Larmor frequency). In principle, even higher frequencies could be in reach by using harmonic frequencies, which are not suppressed. Alternatively, a dedicated board should be designed, similar to Opencore NMR.[32,33]

2.2.3. A permanent magnet reaching a homogeneity of 0.1 ppm (NMR linewidth)

From the engineering point of view, the most challenging part for a low-field spectrometer is the permanent magnet. While magnetic fields of 1 T can be generated with very small assemblies,[44] it remains a huge challenge to guarantee a homogeneity, which allows NMR linewidths in the Hz-range for spectroscopy. Also, our system should be compatible with a standard NMR tube size of 5 mm in diameter, rather than a microcapillary excited by micro-coils. The know-how for the fabrication of such magnets and the necessary passive and active shims are difficult to find in scientific publications and are rather kept inside commercial companies (namely the different manufacturers of benchtop NMR spectrometers). We have evaluated different providers, which offer a magnet/shim system that achieves a linewidth of 0.1 ppm for a magnet system ranging from 0.5 – 1.5 T.

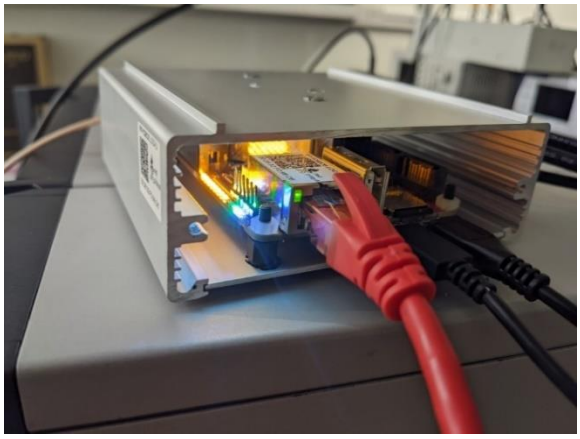

Figure 3. SDRLab 122-16 (Red Pitaya) with Ethernet connection to PC (red), power supply and USB connection to PC. The home-made grey metal case acts as a heat sink for the FPGA and the CPU.

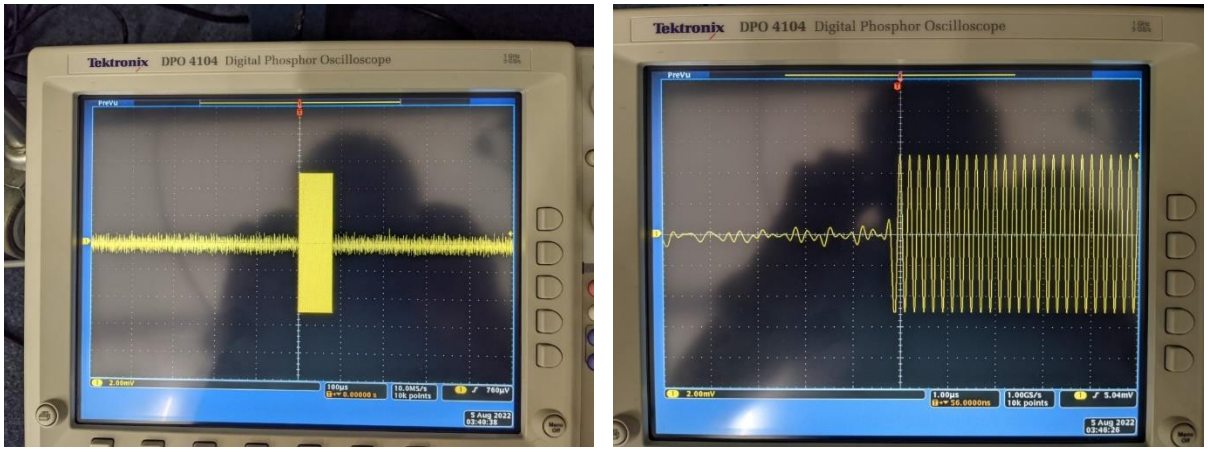

Figure 4. RF pulse (at 24.46 MHz for 80 µs) generated by the SDRLab 122-16 (Red Pitaya) and detected by an oscilloscope, where the frequency and the pulse length were confirmed to be precise. The right screen shows the time axis in units of 100 µs, the left screen in units of 1 µs.

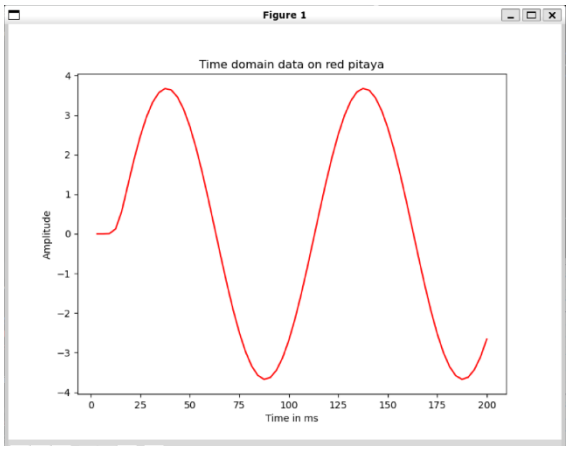

Figure 5. Complex RF signal detected on the SDRLab 122-16/MaRCoS when feeding in an AC RF signal at 5.01 MHz and setting the local oscillator frequency (i.e., the "NMR carrier frequency") at 5 MHz. The plot shows the time domain signal, oscillating with a period of 100 ms, corresponding to the down-converted signal of 10 kHz. The plot shows only the real part, while the SDRLab 122-16 detects the complex data. The first few data points should be discarded, since the detector needs a few milliseconds to start.

In August 2022, we ordered a 0.6 T prototype magnet (^{1}H NMR at 25 MHz) with a homogeneous volume of min. 100 μL (Ø5mm NMR tube), homogeneity corresponding to a linewidth of 0.1 ppm (i.e., 2.5 Hz) from SABR, LLC (USA),[45] where the active shims will be constructed by NuevoMR (USA).[46] A key challenge for permanent magnets is the strong temperature dependence of the magnetic field: neodymium-iron-boron magnets have a field dependence of 1300 ppm/K (personal communication, SABR, LLC, August 10, 2022). This means that only a change of a ΔT = 1 mK will induce a wider shift than the spectral width of 10 ppm for a ^{1}H NMR spectrum. To reduce this strong temperature dependence, SABR will produce the magnet using temperature-compensated samarium-cobalt magnets from the Electron Energy Corporation,[47] which will decrease the temperature dependence of our spectrometer to 50 ppm/K. In practice, a temperature change of up to ΔT = 0.1 K, corresponding to a shift in 5 ppm, will still allow to observe a water signal within the conventional detection bandwidth. The shim coils will be built up by a collection of straight wires, which can be placed within a very thin layer (1 mm in our magnet design).[48] The challenges are that the different orders, in contrast to conventional NMR shim coils, depend on each other, which will make a new approach for automated shimming necessary. The whole magnet has a compact size of roughly 10 cm x 10 cm x 10 cm and weighs less than 5 kg. The gap has a size of 10 mm, which should allow enough space for a 5 mm tube and a RF coil. A drawing of the magnet is given in Figure 6. With a delivery time of 16-20 weeks, the magnet is expected to arrive at ETH Zurich between December 2022 and January 2023. While the development of a prototype costs USD 26,532.00, once established, SABR estimates the cost of a single magnet/active shim system to be USD 8,500.00, for a production quantity of 10 pieces. The largest unknown are the rising material costs in the current global economical situation.

2.2.4. Sensitivity, resolution and price: magnetic field dependence

The key parameters, responsible for the spectral quality and chemical information content, are the SNR ("sensitivity") and the spectral resolution. It is well-known in the NMR literature that the SNR is proportional to ${B_0}^{3/2}$, where B_0 is the static magnetic field.[15] However, this is true for thermal Boltzmann polarization, which scales with B_0. In the case of hyperpolarization, the non-thermal spin polarization becomes independent of the magnetic field, which leads to SNR $\approx {B_0}^{1/2}$. Therefore, for hyperpolarized NMR, SNR still increases with higher magnetic fields, but this dependence is much weaker than for "conventional" NMR relying on thermal Boltzmann polarization. The photo-CIDNP enhancement itself is field dependent, since it is a function of the difference in *g*-values for the dye radical and the molecular (here tryptophan) radical.[8] Torres et al. showed experimentally that for photo-CIDNP on tryptophan using fluorescein as a dye the enhancement was 225 at 200 MHz ^{1}H NMR frequency and 53 at 600 MHz. Based on simulations, it was shown that the maximum photo-CIDNP polarization of this molecule/dye pair is expected at even lower fields, around 1 T. This underlines the important choice of the dye for a given molecule to maximize the photo-CIDNP enhancement for the magnetic field of measurement.

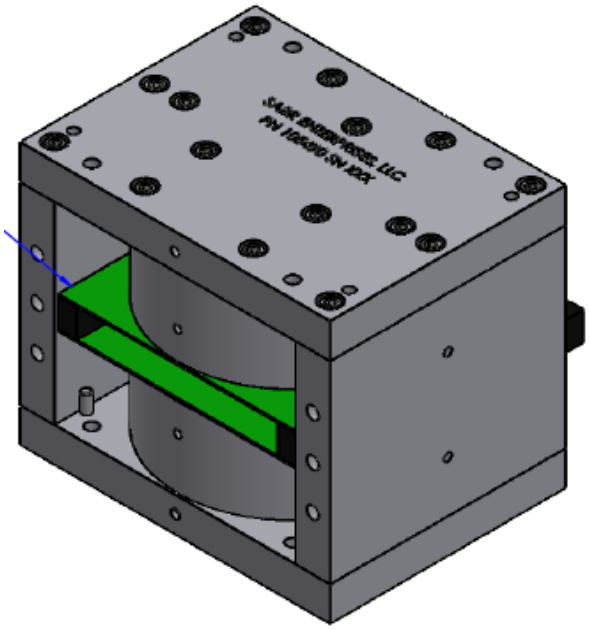

Figure 6. Drawing of the 0.6 T magnet (25 MHz ^{1}H Larmor frequency) ordered at SABR Enterprises, LLC. The green are the layers reserved for passive and active shims, leaving a vertical gap of 10 mm. The length of the magnet is 108 mm. The magnetic field is oriented vertically, perpendicular to the principal axis of the sample tube. This will allow to use solenoid coils for RF excitation/detection.

For the resolution, we should discriminate two meanings, which can be confused. First, resolution stands for the spectral resolution, i.e., linewidth ($1/T_2$*, where T_2* is the decay time of the free induction decay, FID), which is due to the homogeneity of the magnetic field. This is specified by our magnet manufacturer as 0.1 ppm, corresponding to 2.5 Hz at 25 MHz. Second, resolution in NMR language is rather used as the resolution of chemical shifts, i.e., the differences in chemical shifts with respect to *J*-couplings or linewidth. The chemical shifts are proportional to the magnetic field B_0. This is illustrated in a predicted/simulated NMR spectra of the photo-CIDNP-active amino acid tryptophan for three different fields (25, 80 and 300 MHz ^{1}H NMR frequency) in Figure 7. The expected ^{1}H NMR signal for our initial 0.6 T magnet (25 MHz ^{1}H NMR frequency) can be seen on top. By increasing the magnet strength to ca. 1.5 T (80 MHz ^{1}H NMR frequency) is given in the middle, where many more peaks can be recognized. Finally, the spectrum is shown at a "conventional" high-field superconducting magnet of ca. 20 T (600 MHz ^{1}H NMR frequency). For all spectra a linewidth of 2.5 Hz was assumed. This illustrates that any increase of the magnetic field from the starting point of 0.6 T would increase the chemical shift resolution. However, if the relative homogeneity of 0.1 ppm would remain, the linewidth at 80 MHz would become 8 Hz and the whole advantage would vanish. By evaluating the performance of our first 0.6 T (0.1 ppm homogeneity) magnet, we will decide on the optimal specifications for a second magnet. This must include the price for the magnet material, where the amount of magnet material increases quadratically with increasing magnetic field (personal communication, SABR, LLC, August 10, 2022).

In summary, in our preliminary research we have shown that photo-CIDNP efficiently polarizes small aromatic molecules at low fields and make concentrations in the low millimolar to sub-millimolar range detectable within

a few scans. For our low-field NMR spectrometer, we have selected and tested a compact, cheap and versatile console with existing software for MRI applications: MaRCoS running on the SDRLab 122-16 (Red Pitaya). And we have evaluated and ordered a permanent magnet with active shimming system guaranteeing an NMR linewidth of 0.1 ppm (2.5 Hz) for our first low-field spectrometer prototype at 0.6 T / 25 MHz (^{1}H NMR frequency).

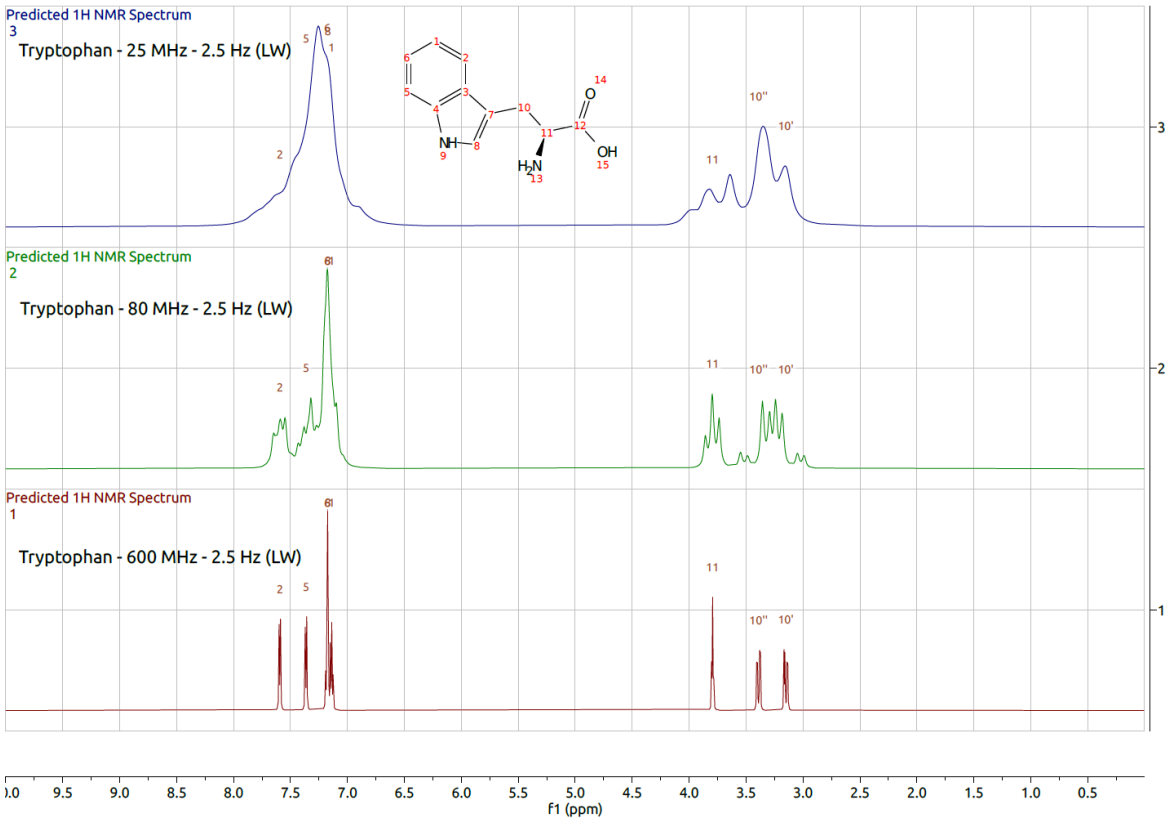

Figure 7. Simulation/prediction ^{1}H NMR spectra using MNova (Mestrelab Research, Spain)[49] of the photo-CIDNP-active amino acid tryptophan (see inset) at three different magnetic fields, corresponding to 600 MHz, 80 MHz and 25 MHz ^{1}H NMR frequencies. The linewidth was set to 2.5 Hz. The three spectra are normalized and display the thermal Boltzmann polarization (not considering the photo-CIDNP effect). The solvent water signal is missing and water exchangeable protons are excluded.

2.3. Detailed research plan

The goal is to construct two prototypes of a low-field (0.5 – 1.5 T) NMR spectrometer with a built-in high-power LED for photo-CIDNP signal enhancement. As evaluated in section 2.1.3, photo-CIDNP is the simplest, cheapest and still very efficient method to hyperpolarize dissolved molecules in low-field NMR. Our spectrometer remains open to be combined with any other hyperpolarization technique, namely SABRE,[23] provided that *p*-H_2 can be produced in a cheap way. After completing this project stage, the spectrometer production costs should be within CHF 10'000.

Our spectrometer will be designed for two types of users:

1. The first type of user includes undergraduate students in an NMR practical course, has no background in NMR. For this user, we preinstall a few standard experiments ("dark" – without photo-CIDNP and "with light" – with photo-CIDNP), which can be run via a simple graphical user interface (GUI), where clicking of a "Start" button is sufficient to launch an experiment. Here, a stable automatization of preparative tasks like shimming or pulse calibration will play a crucial role (see discussion below).
2. The second type of user has a background in NMR and wishes to implement his own pulse sequences. This user will fully profit from the open-source software and the possibility to edit pulse sequences as general and convenient as possible.

While the first prototype spectrometer will be controlled from a PC/notebook, the second prototype will be controlled via a smartphone app, where experiments can be launched, data processed and spectra displayed. The app will be first implemented on the Android system, since this is dominating in the "Global South".[50] Optionally, the app will be also implemented in iOS for iPhones.

The first prototype will be built around the 0.6 T permanent magnet (0.1 ppm/2.5 Hz linewidth) for a 25 MHz ^{1}H NMR spectrometer. By evaluating the results from this first prototype spectrometer, we will order a second magnet (e.g., having a higher field, higher homogeneity, larger sample volume, etc.). Besides these efforts in hardware and software, a focus for the second half of the project lies on experimental and processing-based approaches to simplify the NMR spectra (see spectral overlap in Figure 7) and to extract the maximum of chemical information despite the low magnetic field. Finally, potential experimental applications (for education or research) on our low-field photo-CIDNP spectrometers are evaluated. Importantly, many applications such as those based on a change in the photo-CIDNP effect (competition experiments, see below), do not rely on spectral resolution, but only on the intensity change of the signal.

- The spectrometer will be built by the PhD student under the supervision of the applicant and the project partner (Prof. Roland Riek). The PhD student will have a background in physics, electronic engineering, quantum engineering or physical chemistry. The project will strongly benefit from the specific NMR know-how in our Institute, the Laboratory of Physical Chemistry at ETH Zurich, including the expertise of the electronics workshop (Mr. Tiago Ferreira das Neves and Mr. Alexander Däpp) and the machine workshop (Mr. David Stapfer). With Prof. Peter Güntert and Dr. Piotr Klukowski, the Riek group includes a strong software subgroup with large expertise in NMR-related machine learning,[51] which is a key resource for related topics in our project (see below for details).
- As a preliminary test setup, we can access a magspec (Pure Devices)[30] educational MRI scanner from the research group of Prof. Sebastian Kozerke (Institute for Biomedical Engineering, ETH and University of Zurich), which operates at a very similar frequency (ca. 0.55 T). The magspec can help to test our console, switch and preamplifier (details, see below).
- The Riek group is expected to receive a Fourier 80 benchtop NMR spectrometer (Bruker)[18] as a loan. This will be used as a benchmark for our low-field spectrometer regarding sensitivity, resolution and

for the study of photo-CIDNP field dependence (including 200 and 600 MHz NMR spectrometers with photo-CIDNP access).

2.3.1 Spectrometer hardware

Besides the console (SDRLab 122-16, see section 2.2.2) and the permanent magnet (custom-ordered magnet from SABR, LLC, see section 2.2.3) the following hardware components will complete the spectrometer.

Low-noise amplifier

Between the RF probe (coil) and the RF receiver channel on the console, a low-noise amplifier (LNA), also called preamplifier, will be needed to specifically enhance the signal against the noise. For our RF frequency range, priceworthy products are available from specialized companies, such as Mini-Circuits (USA). The key specification is the noise figure in dB, which should be as low as possible to minimize the noise (and therefore increase the SNR).

- ZFL-500LN+ (Mini-Circuits): With a noise figure of 2.9 dB (at 50 MHz), this is the best connectorized LNA (0.1 - 500 MHz) and costs about USD 100.[52]
- PHA-13LN+ (Mini-Circuits): With an even noise figure of 1.2 dB (at 20 MHz), this is the best non-connectorized LNA (1 - 1000 MHz) and costs about USD 10 (minimum order 20 pieces).[53] A detailed description of the circuit is available from the Martinos Center.[54]

If needed, we will also add an RF amplifier between console output and probe (available again on Mini-Circuits).

Transmit-receive switch

An NMR spectrometer needs an RF switch, which let's the strong RF excitation pulse to the probe, but filters only the weak FID signal to the detection channel.[55] This is challenging, since the FID signal is orders of magnitude weaker than the excitation pulse, but resonates at the identical frequency. We will construct a passive transmit/receive circuit with 3 stage π-networks, which should work efficiently in a range of (ca. 10 – 350 MHz). This design has the advantage that it does not rely on physical quarter-wave cables. The design is adapted from a passive broadband switch in a Varian NMR spectrometer.

RF probe and coil

As it can be seen from Figure 6, to excite the nuclear spins with a magnetic field perpendicular to the static magnetic field B_0, a solenoid coil will be sufficient. This will be first defined for ^{1}H NMR, which could still excite ^{19}F NMR, depending on the tunability of the LC-circuit. For the probe, inspired from magspec (Pure Devices, Germany)[30], we imagine a 3D-printed cartridge/cassette that can host a coil former, where the solenoid coil can be wrapped around. In a later stage "hetero-nuclear" coils for ^{13}C or other nuclei or double resonance coils (e.g., ^{1}H and ^{13}C) could be implemented.

Magnet and active shimming

The most critical point for the magnetic field is the temperature stabilization. We will design a *low-budget* and efficient way to stabilize the temperature of the magnet. This may include thermal insulation, magnet heating (the simplest way of temperature control, also applied in magspec from Pure Devices),[30] or general temperature

control using thermoelectric cooling with a Peltier device. We would add a temperature sensor (for example a platinum temperature sensor) to observe the magnet temperature. This temperature data will be also used for an initial field/frequency locking. For the active shimming, a 32-channel current source will be still needed to build to feed the 32-channel matrix shims.

LED light excitation for photo-CIDNP

We will integrate the LED light excitation for photo-CIDNP into our spectrometer. As high-power LEDs, we will buy the whole spectral range offered by XP-E series (CREE LED, USA),[56] as successfully implemented by Bernarding et al.[29] The drawback of this high-power LEDs are the heating. We will design a way to insulate this from the magnet or keep the LED on during the experiment (continuous heating power) by gating the light using a mechanical switch. The LED or the this switch will be triggered through at TTL signal from the Tx gate of the SDRLab (see Figure 1), which is currently used for gradient control in the MaRCoS MRI.

2.3.2 Spectrometer software

As it is illustrated in Figure 1, the MaRCoS server (C++ on the SDRLab) and the MaRCoS client (Python on PC) already do exist. We will evaluate, how these two types of software have to be adapted for our NMR spectrometer. The NMR data files could be adjusted to the Opencore NMR format,[57] which would make it compatible with its existing processing software. This has furthermore the advantage, not to create one more type of NMR data file. In a second round, the control and processing software will be implemented as a smartphone app on the Android system. This needs a porting of the Python and the MaRCoS client library to the Android system and a GUI for the smartphone for upload of basic sequences and display of recorded spectra.

2.3.3 Automated processes

Users of our low-budget NMR spectrometer do not need to be NMR experts (yet). Therefore, for a convenient and approachable access, some standard procedure, needed to acquire an NMR spectrum, should be automated.

Shimming

Today's high-field NMR spectrometers include an automated shimming based on an optimization algorithm (today, mostly "gradient shimming").[58] This algorithm cannot be used for our spectrometer since it does not contain pulsed field gradients and because the different gradient orders do depend on each other in our thin-layer active shimming system.[48] Therefore, a novel approach for an automated shimming of our setup must be developed. We will consider a very recent deep-learning based approach,[59] which could be implemented in a collaboration with Dr. Mazin Jouda and Prof. Jan Korvink from KIT, Germany. The large experimental data sets (1D ^{1}H spectra at different shim settings), needed to train the model, will be recorded in an automated manner.

Locking

In conventional liquid-state NMR spectrometers, the field/frequency lock is guaranteed by measuring a deuterium NMR signal of an added deuterated solvent (e.g., 10 % D_2O when measuring in H_2O). Since deuterated chemicals are expensive and not easily accessible to researchers of the "Global South", we will not rely on this locking scheme. In a first step, we will measure the magnet temperature, which will be calibrated to its magnetic field, already giving a rough idea, where the RF carrier frequency has to be set. In a second step, the strongest

signal from the water solvent will be detected and the field/frequency will be locked on it. In case of using for example organic solvents, the solvent frequency can be adjusted (as this is done for deuterated solvents in the deuterium lock of standard NMR spectrometers).

Pulse calibration and water suppression

Preparatory steps like pulse calibration (determination of optimal pulse length for a given pulse power), will be also automated, by recording a Rabi oscillation and taking its Fourier transform or fitting a cosine function to the time signal. Water suppression will be implemented as a presaturation, also using composite pulses, as successfully demonstrated using the Fourier 80 spectrometer (see Figure 2). An alternative approach consists of a selective inversion of the water signal, followed by a delay fixed to the zero-crossing of water. This may be preferential to reduce dynamic range issues.

2.3.4 Spectral simplification

As it is evident from the predicted/simulated low-field NMR spectrum at 0.6 T (see Figure 7), the strong spectral overlap makes chemical structure analysis challenging. To improve the spectral quality and to extract the maximum information content of it, we will work on experimental and processing approaches, which will specifically address the challenges of low-field NMR spectroscopy. The ultimate line broadening will be given by the magnetic field drift during the acquisition time of a single scan (around one second). The FID should contain a characteristic frequency-modulated "chirp" contribution, which could be demodulated in a processing step. We will explore, how much the spectral line could be narrowed by applying this process. Ideally, this step would give us the chance to profit from prolonged transverse relaxation times T_2 or T_2* at low magnetic fields.

A classic way to reduce the complexity of NMR spectra is decoupling, where a *J*-multiplets are reduced to a single line, increasing resolution and sensitivity at the same time. While heteronuclear decoupling (removing *J*-couplings of ^{1}H spins to ^{13}C or other nuclei) is simply implemented by a continuous-wave irradiation of the coupled nuclei, homonuclear decoupling is challenging, since all observed nuclei have the same resonance frequency. Many of the elegant solutions of homonuclear decoupling rely on pulsed field gradients,[60] which cannot be implemented on our low-field spectrometer. Polychromatic decoupling,[61] where a number of resonances can be decoupled through a gated acquisition sequence. In a similar way, spin tickling can be implemented to study the connectivities.[62] Of course, two-dimensional (2D) NMR is one of the most elegant way to solve the resolution issue. 2D NMR can be implemented on our spectrometer, but might be challenging in combination with photo-CIDNP due to bleaching of the dye. An alternative is "virtual decoupling", where the *J*-multiplets are evolved into in-phase or anti-phase for different scans, which are then combined to find the central frequency.[63,64] Very recently, virtual homonuclear decoupling was successfully performed as a processing step relying on deep neural networks by Flemming Hansen's group: a single 1D ^{1}H spectrum is sufficient as an input to generate a decoupled spectrum.[65] This shows the strength of neural networks for NMR processing. Along these lines, we plan to collaborate with Prof. Hansen to generate "high-field" spectra from "low-field" spectra (going from top to bottom in Figure 7) by training neural networks on a large spectral data set, collected at different Larmor frequencies for photo-CIDNP and "dark" NMR spectra data sets.

2.3.5 Potential applications on the low-field photo-CIDNP NMR spectrometer

We will test different applications, which could be used for education or research on the low-field photo-CIDNP NMR spectrometer with a focus on biological applications and drug screening.

Photo-CIDNP-based drug screening

Research

Our spectrometer will allow for photo-CIDNP-based drug screening. Photo-CIDNP-active ligands, small molecules or "fragments", will be tested in absence and presence of a target protein under light illumination. At low-field ^{1}H NMR (25 MHz or higher), the hyperpolarized ligand will be the only signal visible besides the solvent signal from water. In case of a binding event of the small molecule to the protein, the photo-CIDNP effect will decrease, resulting in an NMR signal decrease, since the molecule becomes less accessible to the excited dye molecule, reporting a "binding hit". Importantly, this type of experiment does not suffer from the limited resolution (small chemical shift dispersion), since only the intensity change is recorded. For this reason, this application is ideally suited for our spectrometer with good sensitivity (thanks to the photo-CIDNP enhancement) despite its limited resolution.

Education

For educational purposes, an ideal protein-ligand pair is bovine serum albumin (BSA), a cheap and readily available protein, and the amino acid tryptophan as ligand with a dissociation constant $K_d \approx 60$ μM.[66,67] Tryptophan can be efficiently polarized through photo-CIDNP using the cheap and readily available fluorescent dye fluorescein (excitation with blue light around 450 nm).[12] The addition of BSA will decrease the photo-CIDNP NMR signal of tryptophan, reporting a "binding hit" for this protein-ligand pair. Since human serum albumin (HSA) acts as a reservoir and transport protein in the blood, binding of drugs to albumin in humans play a key role for the pharmacokinetic properties, which underlines the pharmacological relevance of such an educational laboratory experiment.[68]

Photo-CIDNP-based drug screening via competitive binding

Research

As it was highlighted by Torres et al.,[8] a maximal photo-CIDNP effect is observed for a specific combination of 1) a dye molecule, 2) a molecule of interest and 3) the magnetic field strength. Therefore, an efficient approach would be to keep an "ideal pair" of dye and molecule (e.g., fluorescein and tryptophan with the protein albumin), which leads to a strong NMR signal enhancement at our magnetic field. Based on this pair, competition experiments could be performed, by screening different potential ligands against the small molecule (e.g., tryptophan), in the presence of a protein of interest. As long as tryptophan binds to the protein, its ^{1}H NMR signal remains weak. However, if an added molecule would outperform tryptophan by binding stronger to the protein albumin, this would lead to a recovery of the photo-CIDNP enhanced ^{1}H NMR of tryptophan, generating a "binding hit" for the small molecule. This optimized condition would allow to lower the concentration of the ligands and the protein. And even more important, the screened molecules of interest (potential ligands) do not have to be photo-CIDNP active, which opens the chemical space to all small molecules beyond aromatic systems.

Education

The principle of competitive binding is a major concept in drug discovery as it is also used with radioactive ligands (radiotracer) to identify competitive binders.[69] Educational experiments based on photo-CIDNP drug screening via competitive binding will enable to teach students in pharmaceutical studies the underlying principles without depending on expensive radiotracers.

Identification of photo-CIDNP-active molecules

Research

A brute-force approach will be the measurement of natural product extracts with and without photo-CIDNP. This could be samples like coffee or tea from food science, but can be extended to local medicinal herbs. Positive results, the "hit" of one or several photo-CIDNP active compounds, will lead to the extension of the currently known photo-CIDNP molecule library and could also mark the starting point for the discovery of unknown natural or metabolic compounds. The chemical analysis of the substances will be carried out on one hand using experimental, processing and neural network-based spectral simplification (see section 2.3.4). On the other hand, samples can be shipped to ETH Zurich to conduct further chemical analysis, building up an international collaboration.

2.3.6 Initial partnership with a university of the "Global South"

Towards the end of the project, we will establish a collaboration with a university of the "Global South" (for example in an African country) and deliver one of our protypes to the institution. A researcher or PhD student from the collaboration partner will be invited to ETH Zurich, to learn all about the light-enhanced low-field NMR spectrometer and the photo-CIDNP based drug screening applications or one of our scientists will accompany the spectrometer to a give a training at the site of the collaboration partner. Basic chemicals for the photo-CIDNP screening like fluorescein or protein targets will be supplied. For this initial know-how transfer, we will profit from the experience of ETH for Development (ETH4D) at ETH Zürich.

2.4. Schedule and milestones

Activity	Month 1-6	7-12	13-18	19-24	25-30	31-36	37-42	43-48
Construction of low-field photo-CIDNP NMR spectrometer #1	x	x						
Automatization of NMR experimental processes		x	x					
Development of a Smartphone app for spectrometer control				x				
Publications				x				x
Construction spectrometer #2 at a higher field					x	x		
Experimental and processing methods for spectral simplification			x			x		
Experimental applications for the low-field photo-CIDNP spectrometer						x	x	
Initial partnership with a university from the "Global South"								x

2.5. Relevance and impact

Scientific relevance

We envision that our low-budget light-enhanced NMR spectrometer will become a new tool for teaching magnetic resonance in general. Today, almost all liquid-state NMR spectrometers have become commercial devices. For the vast majority of the users, NMR spectrometers have become a black box, which turns their molecule inside a sample tube into an NMR spectrum (or, more recently, even directly into a chemical structure). In strong contrast, all parts of our spectrometers are visible and accessible, the software is open source. Our device is therefore ideally suited to teach the functioning of an NMR spectrometer from scratch and will be used in the "Praktikum" for chemistry students. While a few basic NMR (simple pulse experiment, Hahn echo, inversion recovery, etc.) and photo-CIDNP experiments will be implemented as plug-and-play experiments, at the same time, our open-source approach will allow advanced users to create their own photo-CIDNP and conventional pulse NMR sequences. Importantly, we see our development as a challenge, to push down the cost limits and explore the information content of low-field NMR spectroscopy in combination with photo-CIDNP signal enhancement.

We will publish all our results in fully open-access journals. We plan at least three publications by covering 1) the technical details (hard- and software) of the device and 2) applications based on our light-enhanced spectrometer and 3) the neural network-based efforts of simplifying and analyzing low-field spectra. An option for a fourth publication could be the role of our spectrometer as an educational tool for high school and university practical courses. An ideal platform for these manuscripts would be the open-access and not-for-profit international journal "Magnetic Resonance",[70] which was founded in 2020 by the Groupement AMPERE, an association of NMR scientists. Detailed data on the spectrometer itself (plans, software, tutorials, etc.) will be published on a public internet homepage, where a public forum will allow for discussions and potential collaborations.

Broader impact

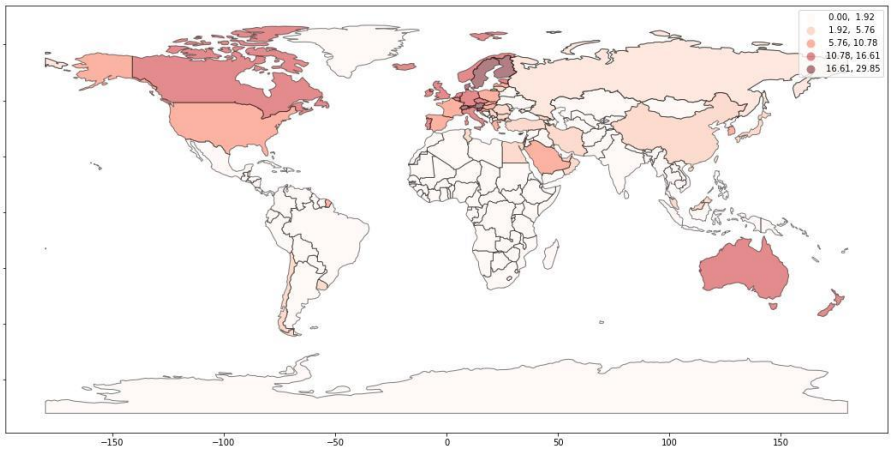

Figure 8. The NMR world map: Origin of NMR publications per capita. All NMR publications from Scopus in the year 2021 were divided by 1 million inhabitants. White countries have no access to NMR, while Switzerland is the global NMR world leader. (Dr. Maria Pechlaner, Infozentrum Chem. Biol. Pharm., ETH Zürich.)

Nuclear Magnetic Resonance (NMR) spectroscopy is one of the most versatile and powerful analytical tool for chemistry, biology, pharmaceutical or material sciences. At the same time, NMR is an ideal playground to experience quantum mechanics "with own hands": NMR (and subsequently MRI) was the first application originating from quantum mechanics. NMR spectroscopy uses very strong (up to 30 T) and highly homogeneous magnetic fields, which are generated by low-temperature super-conducting magnets. Only this guarantees the essential combination of high spectral resolution and sufficient sensitivity. Besides the high acquisition costs of such a device, the maintenance costs for liquid Helium cooling are very expensive and its scarcity on the market is becoming a practical challenge. Therefore, high-field NMR spectrometers are commonly found only in the countries of the "Global North".

Our project

Our goal is to produce an NMR spectrometer for CHF 10'000. We envision that our low-budget light-enhanced NMR spectrometer will become an accessible tool for students and researchers in academic institutions of the "white countries" in the Figure 8 above. Thereby, the spectrometer can be operated in the "dark mode" without light-enhanced photo-CIDNP using high concentration of dissolved molecules (e.g., ethanol, > 1 mM) or in the "light mode" profiting from photo-CIDNP hyperpolarization. In the "dark mode", the spectrometer will be a tool to gain experimental insights on the key features of quantum physics such as quantum states, coherent superpositions, couplings, qubits, relaxation and dynamical decoupling.[71,72] Such an early confrontation, ideally already during the undergraduate studies, will increase the students' awareness for the key features of quantum physics, which are the ingredients of today's second quantum revolution[73] in fields like quantum computing, communication or sensing. In the "light mode", biological (and potentially further) applications of photo-CIDNP NMR spectroscopy can be performed with our low-field NMR spectrometer. As one example, protein-ligand binding can be studied using a competition experiment:[13] The structural identification of these substances could be completed in collaboration with research groups at ETH Zurich.

Our final product is more than the spectrometer with its hard- and software alone: it is an open source community of developers and users with new ties from academic institutions of the "Global South" to the "Global North". For once, this is not competition-driven but rather cooperation-driven science, where any interested researcher can contribute. Members of the community will reply to questions, repair parts or fix bugs and support the development of new experiments and applications. Replacement parts will be shipped from ETH Zurich. Not relying on cryogenics our magnet will be an environmentally sustainable NMR spectrometer with negligeable operating costs.

The applicant acknowledges stimulating discussions with Dr. Albannay Mohammed (ETH Zürich, now Quad Systems Ltd., Dietlikon, Switzerland), Prof. Matthias Ernst (LPC, ETH Zürich), Dr. Félix Torres (LPC, ETH Zürich and NexMR GmbH, Schlieren), Prof. Sebastian Kozerke (D-ITET, ETH Zürich), Prof. Bernhard Blümich (RWTH Aachen, Germany), Dr. Mazin Jouda (KIT, Germany), Prof. Jan Korvink (KIT, Germany), Prof. Kazuyuki Takeda (Kyoto University, Japan), Dr. Vlad Negnevitsky (Oxford Ionics, UK), Dr. Juan Parra-Robles (Cincinnati Children's Hospital Medical Center, USA) and Dr. Andrew McDowell (NuevoMR, USA).

3. Bibliography

(1) Kaptein, R.; Dijkstra, K.; Nicolay, K. Laser Photo-CIDNP as a Surface Probe for Proteins in Solution. *Nature* **1978**, *274* (5668), 293–294. https://doi.org/10.1038/274293a0.

(2) Im, J.; Lee, J.; Lee, J. H. Surface Accessibility of an Intrinsically Disordered Protein Probed by 2D Time-Resolved Laser-Assisted NMR Spectroscopy. *J. Am. Chem. Soc.* **2022**. https://doi.org/10.1021/jacs.2c06309.

(3) Hore, P. J.; Broadhurst, R. W. Photo-CIDNP of Biopolymers. *Prog. Nucl. Magn. Reson. Spectrosc.* **1993**, *25*, 345–402. https://doi.org/10.1016/0079-6565(93)80002-B.

(4) Shapira, B.; Morris, E.; Muszkat, K. A.; Frydman, L. Sub-Second 2D NMR Spectroscopy at Sub-Millimolar Concentrations. *J. Am. Chem. Soc.* **2004**, *126* (38), 11756–11757. https://doi.org/10.1021/ja0461668.

(5) Sekhar, A.; Cavagnero, S. ^{1}H Photo-CIDNP Enhancements in Heteronuclear Correlation NMR Spectroscopy. *J. Phys. Chem. B* **2009**, *113* (24), 8310–8318. https://doi.org/10.1021/jp901000z.

(6) Lee, J. H.; Okuno, Y.; Cavagnero, S. Sensitivity Enhancement in Solution NMR: Emerging Ideas and New Frontiers. *J. Magn. Reson.* **2014**, *241* (1), 18–31. https://doi.org/10.1016/j.jmr.2014.01.005.

(7) Sobol, A.; Torres, F.; Aicher, A.; Renn, A.; Riek, R. Atto Thio 12 as a Promising Dye for Photo-CIDNP. *J. Chem. Phys.* **2019**, *151* (23), 234201. https://doi.org/10.1063/1.5128575.

(8) Torres, F.; Sobol, A.; Greenwald, J.; Renn, A.; Morozova, O.; Yurkovskaya, A.; Riek, R. Molecular Features toward High Photo-CIDNP Hyperpolariztion Explored through the Oxidocyclization of Tryptophan. *Phys. Chem. Chem. Phys.* **2021**, *23* (11), 6641–6650. https://doi.org/10.1039/d0cp06068b.

(9) Torres, F.; Renn, A.; Riek, R. Exploration of the Close Chemical Space of Tryptophan and Tyrosine Reveals Importance of Hydrophobicity in CW-Photo-CIDNP Performances. *Magn. Reson.* **2021**, *2* (1), 321–329. https://doi.org/10.5194/mr-2-321-2021.

(10) Mompeán, M.; Sánchez-Donoso, R. M.; De La Hoz, A.; Saggiomo, V.; Velders, A. H.; Gomez, M. V. Pushing Nuclear Magnetic Resonance Sensitivity Limits with Microfluidics and Photo-Chemically Induced Dynamic Nuclear Polarization. *Nat. Commun.* **2018**, *9* (1), 1–8. https://doi.org/10.1038/s41467-017-02575-0.

(11) Lee, J. H.; Cavagnero, S. A Novel Tri-Enzyme System in Combination with Laser-Driven NMR Enables Efficient Nuclear Polarization of Biomolecules in Solution. *J. Phys. Chem. B* **2013**, *117*, 6069–6081. https://doi.org/10.1021/jp4010168.

(12) Okuno, Y.; Cavagnero, S. Fluorescein: A Photo-CIDNP Sensitizer Enabling Hypersensitive NMR Data Collection in Liquids at Low Micromolar Concentration. *J. Phys. Chem. B* **2016**, *120* (4), 715–723. https://doi.org/10.1021/acs.jpcb.5b12339.

(13) Torres, F.; Bütikofer, M.; Riek, R. Ultrafast structure activity relationship by photo-CIDNP NMR spectroscopy (ETH Spark Award – Top 5) https://ethz.ch/en/industry/researchers/ip/sparkaward/2022.html (accessed Sep 8, 2022).

(14) Torres, F. NexMR - Starting off on the right molecules www.nexmr.com (accessed Sep 8, 2022).

(15) Webb, A. Increasing the Sensitivity of Magnetic Resonance Spectroscopy and Imaging. *Anal. Chem.* **2012**, *84* (1), 9–16. https://doi.org/10.1021/ac201500v.

(16) Blümich, B. Low-Field and Benchtop NMR. *J. Magn. Reson.* **2019**, *306*, 27–35. https://doi.org/10.1016/j.jmr.2019.07.030.

(17) Magritek. Magritek - Spinsolve family https://magritek.com/products/benchtop-nmr-spectrometer-spinsolve/ (accessed Sep 8, 2022).

(18) Bruker. Bruker - Fourier 80 https://www.bruker.com/en/products-and-solutions/mr/nmr/fourier80.html (accessed Sep 8, 2022).

(19) Q Magnetics, Q Magnetics - NMR for everyone https://www.qmagnetics.com/contact (accessed Sep 8, 2022).

(20) Castaing-Cordier, T.; Bouillaud, D.; Farjon, J.; Giraudeau, P. Recent Advances in Benchtop NMR Spectroscopy and Its Applications. *Annu. Reports NMR Spectrosc.* **2021**, *103*, 191–258. https://doi.org/10.1016/bs.arnmr.2021.02.003.

(21) Albert, M. S.; Cates, G. D.; Driehuys, B.; Happer, W.; Saam, B.; Springer Jr, C. S.; Wishnia, A. Biological Magnetic Resonance Imaging Using Laser-Polarized Xe-129. *Nature* **1994**, *370*, 199–201.

(22) Parra-Robles, J.; Cross, A. R.; Santyr, G. E. Theoretical Signal-to-Noise Ratio and Spatial Resolution Dependence on the Magnetic Field Strength for Hyperpolarized Noble Gas Magnetic Resonance Imaging of Human Lungs. *Med. Phys.* **2005**, *32* (1), 221–229. https://doi.org/10.1118/1.1833593.

(23) Adams, R. W.; Aguilar, J. A.; Atkinson, K. D.; Cowley, M. J.; Elliott, P. I. P.; Duckett, S. B.; Green, G. G. R.; Khazal, I. G.; Lopez-Serrano, J.; Williamson, D. C. Reversible Interactions with Para-Hydrogen Enhance NMR Sensitivity by Polarization Transfer. *Science* **2009**, *323* (March), 1708–1711.

(24) Richardson, P. M.; Parrott, A. J.; Semenova, O.; Nordon, A.; Duckett, S. B.; Halse, M. E. SABRE Hyperpolarization Enables High-Sensitivity ^{1}H and ^{13}C Benchtop NMR Spectroscopy. *Analyst* **2018**, *143* (14), 3442–3450. https://doi.org/10.1039/c8an00596f.

(25) El Daraï, T.; Cousin, S. F.; Stern, Q.; Ceillier, M.; Kempf, J.; Eshchenko, D.; Melzi, R.; Schnell, M.; Gremillard, L.; Bornet, A.; Milani, J.; Vuichoud, B.; Cala, O.; Montarnal, D.; Jannin, S. Porous Functionalized Polymers Enable Generating and Transporting Hyperpolarized Mixtures of Metabolites. *Nat. Commun.* **2021**, *12*, 4695. https://doi.org/10.1038/s41467-021-24279-2.

(26) Ardenkjaer-Larsen, J. H.; Fridlund, B.; Gram, A.; Hansson, G.; Thaning, M.; Hansson, L.; Lerche, M. H.; Servin, R.; Golman, K. Increase in Signal-to-Noise Ratio of > 10,000 Times in Liquid-State NMR. *Proc. Natl. Acad. Sci.* **2003**, *100* (18), 10158–10163. https://doi.org/10.1073/pnas.1733835100.

(27) Picazo-Frutos, R.; Stern, Q.; Blanchard, J.; Cala, O.; Ceillier, M.; Cousin, S. F.; Eills, J.; Elliot, S. J.; Jannin, S.; Budker, D. Zero- to Ultralow-Field Nuclear Magnetic Resonance Enhanced with Dissolution Dynamic Nuclear Polarization. *ChemRxiv* **2022**. https://doi.org/10.26434/chemrxiv-2022-f8t03-v2.

(28) Keller, T. J.; Laut, A. J.; Sirigiri, J.; Maly, T. High-Resolution Overhauser Dynamic Nuclear Polarization Enhanced Proton NMR Spectroscopy at Low Magnetic Fields. *J. Magn. Reson.* **2020**, *313*, 106719. https://doi.org/10.1016/j.jmr.2020.106719.

(29) Bernarding, J.; Bruns, C.; Prediger, I.; Plaumann, M. LED-Based Photo-CIDNP Hyperpolarization Enables ^{19}F MR Imaging and ^{19}F NMR Spectroscopy of 3-Fluoro-DL-tyrosine at 0.6 T. *Appl. Magn. Reson.* **2022**. https://doi.org/10.1007/s00723-022-01473-z.

(30) Pure Devices. Pure Devices - Research MRI systems https://www.pure-devices.com/index.php/products/products-research/products-research-overview.html (accessed Sep 9, 2022).

(31) Takeda, K. Opencore NMR 2 http://kuchem.kyoto-u.ac.jp/bun/indiv/takezo/opencorenmr2/index.html (accessed Sep 15, 2022).

(32) Takeda, K. A Highly Integrated FPGA-Based Nuclear Magnetic Resonance Spectrometer. *Rev. Sci. Instrum.* **2007**, *78* (3). https://doi.org/10.1063/1.2712940.

(33) Takeda, K. OPENCORE NMR: Open-Source Core Modules for Implementing an Integrated FPGA-Based NMR Spectrometer. *J. Magn. Reson.* **2008**, *192* (2), 218–229. https://doi.org/10.1016/j.jmr.2008.02.019.

(34) Batel, M.; Krajewski, M.; Weiss, K.; With, O.; Däpp, A.; Hunkeler, A.; Gimersky, M.; Pruessmann, K. P.; Boesiger, P.; Meier, B. H.; Kozerke, S.; Ernst, M. A Multi-Sample 94 GHz Dissolution Dynamic-Nuclear-Polarization System. *J. Magn. Reson.* **2012**, *214*, 166–174. https://doi.org/10.1016/j.jmr.2011.11.002.

(35) Takeda, K. Open source imaging - Opencore NMR

https://www.opensourceimaging.org/project/opencore-nmr/ (accessed Sep 15, 2022).

(36) Winter, L. Open Source Magnetic Resonance Imaging: From the Community to the Community. https://www.opensourceimaging.org/.

(37) Negnevitsky, V.; Vives-Gilabert, Y.; Algarín, J. M.; Craven-Brightman, L.; Pellicer-Guridi, R.; O'Reilly, T.; Stockmann, J. P.; Webb, A.; Alonso, J.; Menküc, B. MaRCoS, an Open-Source Electronic Control System for Low-Field MRI. *arXiv* **2022**. https://doi.org/10.48550/arXiv.2208.01616.

(38) Red Pitaya, SDRlab 122-16 https://redpitaya.com/sdrlab-122-16/ (accessed Sep 16, 2022).

(39) OneSDR. How does Software-defined radio (SDR) work? https://www.onesdr.com/2019/10/03/what-is-software-defined-radio-sdr/ (accessed Sep 16, 2022).

(40) Michal, C. A. A Low-Cost Multi-Channel Software-Defined Radio-Based NMR Spectrometer and Ultra-Affordable Digital Pulse Programmer. *Concepts Magn. Reson. Part B Magn. Reson. Eng.* **2018**, *48B* (3), 1–14. https://doi.org/10.1002/cmr.b.21401.

(41) Guallart-Naval, T.; O'Reilly, T.; Algarín, J. M.; Pellicer-Guridi, R.; Vives-Gilabert, Y.; Craven-Brightman, L.; Negnevitsky, V.; Menküc, B.; Galve, F.; Stockmann, J. P.; Webb, A.; Alonso, J. Benchmarking the Performance of a Low-Cost Magnetic Resonance Control System at Multiple Sites in the Open MaRCoS Community. *arXiv* **2022**. https://doi.org/10.48550/arXiv.2203.11314.

(42) Miyanishi, K.; Segawa, T. F.; Takeda, K.; Ohki, I.; Onoda, S.; Ohshima, T.; Abe, H.; Takashima, H.; Takeuchi, S.; Shames, A. I.; Morita, K.; Wang, Y.; So, F. T. K.; Terada, D.; Igarashi, R.; Kagawa, A.; Kitagawa, M.; Mizuochi, N.; Shirakawa, M.; Negoro, M. Room-Temperature Hyperpolarization of Polycrystalline Samples with Optically Polarized Triplet Electrons: Pentacene or Nitrogen-Vacancy Center in Diamond? *Magn. Reson.* **2021**, *2* (1), 33–48. https://doi.org/10.5194/mr-2-33-2021.

(43) Negnevitsky, V. GitHub - Setting MaRCoS up https://github.com/vnegnev/marcos_extras/wiki/setting_marcos_up (accessed Sep 19, 2022).

(44) Blümich, B.; Rehorn, C.; Zia, W. Magnets for Small-Scale and Portable NMR. In *Micro and Nano Scale NMR: Technologies and Systems*; Anders, J., Korvink, J. G., Eds.; Wiley-VCH Verlag GmbH & Co., 2018; pp 1–20. https://doi.org/10.1002/9783527697281.ch1.

(45) Mercurio, R. SABR Enterprises, LLC https://www.sabrllc.net/ (accessed Sep 21, 2022).

(46) McDowell, A. NuevoMR, LLC http://www.nuevomr.com/ (accessed Sep 21, 2022).

(47) Electron Energy Corporation, Temperature compensated Samarium Cobalt Magnets https://www.electronenergy.com/temperature-compensated-samarium-cobalt-magnets/ (accessed Sep 21, 2022).

(48) McDowell, A.; Conradi, M. Thin High-Order Shims for Small Dipole NMR Magnets. *J. Magn. Reson.* **2017**, *281*, 7–16. https://doi.org/10.1016/j.jmr.2017.04.013.

(49) Mestrelab. MNova https://mestrelab.com/software/mnova/ (accessed Sep 23, 2022).

(50) MobileApps.com. Android vs iOS Market Share 2020: Stats and Facts https://www.mobileapps.com/blog/android-vs-ios-market-share (accessed Sep 23, 2022).

(51) Klukowski, P.; Riek, R.; Güntert, P. Rapid Protein Assignments and Structures from Raw NMR Spectra with the Deep Learning Technique ARTINA. *arXiv* **2022**. https://doi.org/10.48550/arXiv.2201.12041.

(52) Mini-Circuits. ZFL-500LN+ https://www.minicircuits.com/WebStore/dashboard.html?model=ZFL-500LN%2B (accessed Sep 23, 2022).

(53) Mini-Circuits. PHA-13LN+ https://www.minicircuits.com/WebStore/dashboard.html?model=PHA-13LN%2B (accessed Sep 23, 2022).

(54) Craven-Brightman, L. Low-noise RF Preamplifier https://rflab.martinos.org/index.php?title=Low-noise_RF_Preamplifier (accessed Sep 23, 2022).

(55) Fukushima, E.; Roeder, S. B. W. *Experimental Pulse NMR: A Nuts and Bolts Approach*, 1st Editio.; CRC Press, 1981. https://doi.org/10.1201/9780429493867.

(56) Mouser. Cree LED XLamp XP-E LEDs https://www.mouser.ch/new/cree/cree-xp-e-leds/ (accessed Sep 23, 2022).

(57) Takeda, K. Opencore NMR - Data Files https://opencorenmr.github.io/opencorenmr-docs/blog/dataFiles/dataFiles.html (accessed Sep 23, 2022).

(58) Weiger, M.; Speck, T.; Fey, M. Gradient Shimming with Spectrum Optimisation. *J. Magn. Reson.* **2006**, *182* (1), 38–48. https://doi.org/10.1016/j.jmr.2006.06.006.

(59) Becker, M.; Jouda, M.; Kolchinskaya, A.; Korvink, J. G. Deep Regression with Ensembles Enables Fast, First-Order Shimming in Low-Field NMR. *J. Magn. Reson.* **2022**, *336*, 107151. https://doi.org/10.1016/j.jmr.2022.107151.

(60) Zangger, K.; Sterk, H. Homonuclear Broadband-Decoupled NMR Spectra. *J. Magn. Reson.* **1997**, *489* (124), 486–489.

(61) Carnevale, D.; Segawa, T. F.; Bodenhausen, G. Polychromatic Decoupling of a Manifold of Homonuclear Scalar Interactions in Solution-State NMR. *Chem. - A Eur. J.* **2012**, *18* (37), 11573–11576. https://doi.org/10.1002/chem.201200481.

(62) Segawa, T. F.; Carnevale, D.; Bodenhausen, G. How to Tickle Spins with a Fourier Transform NMR Spectrometer. *ChemPhysChem* **2013**, *14* (2), 369–373. https://doi.org/10.1002/cphc.201200858.

(63) Sørensen, M. D.; Meissner, A.; Sørensen, O. W. Spin-State-Selective Coherence Transfer via Intermediate States of Two-Spin Coherence in IS Spin Systems: Application to E.COSY-Type Measurement of J Coupling Constants. *J. Biomol. NMR* **1997**, *10* (2), 181–186. https://doi.org/10.1023/A:1018323913680.

(64) Ottiger, M.; Delaglio, F.; Bax, A. Measurement of J- and Dipolar Couplings from Simplified Two-Dimensional NMR Spectra. *J. Magn. Reson.* **1998**, *131* (2), 373–378. https://doi.org/10.1006/jmre.1998.1361.

(65) Karunanithy, G.; Mackenzie, H. W.; Hansen, D. F. Virtual Homonuclear Decoupling in Direct Detection Nuclear Magnetic Resonance Experiments Using Deep Neural Networks. *J. Am. Chem. Soc.* **2021**, *143* (41), 16935–16942. https://doi.org/10.1021/jacs.1c04010.

(66) Fielding, L.; Rutherford, S.; Fletcher, D. Determination of Protein-Ligand Binding Affinity by NMR: Observations from Serum Albumin Model Systems. *Magn. Reson. Chem.* **2005**, *43* (6), 463–470. https://doi.org/10.1002/mrc.1574.

(67) Angulo, J.; Enríquez-Navas, P. M.; Nieto, P. M. Ligand-Receptor Binding Affinities from Saturation Transfer Difference (STD) NMR. *Chem. - A Eur. J.* **2010**, *16* (26), 7803–7812. https://doi.org/10.1002/chem.200903528.

(68) Yamasaki, K.; Chuang, V. T. G.; Maruyama, T.; Otagiri, M. Albumin-Drug Interaction and Its Clinical Implication. *Biochim. Biophys. Acta - Gen. Subj.* **2013**, *1830* (12), 5435–5443. https://doi.org/10.1016/j.bbagen.2013.05.005.

(69) Hulme, E. C.; Trevethick, M. A. Ligand Binding Assays at Equilibrium: Validation and Interpretation. *Br. J. Pharmacol.* **2010**, *161* (6), 1219–1237. https://doi.org/10.1111/j.1476-5381.2009.00604.x.

(70) Magnetic Resonance - An interactive open-access publication of the Groupement AMPERE https://www.magnetic-resonance-ampere.net/.

(71) Jones, J. A.; Hansen, R. H.; Mosca, M. Quantum Logic Gates and Nuclear Magnetic Resonance Pulse Sequences. *J. Magn. Reson.* **1998**, *135* (2), 353–360. https://doi.org/10.1006/jmre.1998.1606.

(72) Freeman, R. Beg, Borrow, or Steal. Finding Ideas for New NMR Experiments. *Concepts Magn. Reson. Part A Bridg. Educ. Res.* **2003**, *17* (1), 71–85. https://doi.org/10.1002/cmr.a.10059.

(73) Trabesinger, A. We are entering the second quantum revolution. This is how we got here. https://ethambassadors.ethz.ch/2020/01/21/we-are-entering-the-second-quantum-revolution-this-is-how-we-got-here/ (accessed Sep 1, 2022).

(74) Blanchard, J. W.; Budker, D. Zero-to Ultralow-Field NMR. *eMagRes* **2007**, *5*, 1395–1410. https://doi.org/10.1002/9780470034590.emrstm1369.